Available online at www.sciencedirect.com
ScienceDirect
Journal of Power Sources 160 (2006) 957–968
JOURNAL OF POWER SOURCES
www.elsevier.com/locate/jpowsour

The stability of Pt–M (M = first row transition metal) alloy catalysts and its effect on the activity in low temperature fuel cells A literature review and tests on a Pt–Co catalyst

Ermete Antolini [a], Jose R.C. Salgado [b], Ernesto R. Gonzalez [a,*]

[a] *Instituto de Química de São Carlos, USP, C.P. 780, São Carlos, SP 13560-970, Brazil*
[b] *Instituto de Química, UnB, C.P. 4478, Brasília, DF 70919-970, Brazil*

Received 8 February 2006; received in revised form 2 March 2006; accepted 3 March 2006
Available online 18 April 2006

Abstract

Carbon supported platinum metal alloy catalysts (Pt–M/C) are widely used in low temperature fuel cells. Pt alloyed with first-row transition elements is used as improved cathode material for low temperature fuel cells. A major challenge for the application of Pt–transition metal alloys in phosphoric acid (PAFC) and polymer electrolyte membrane (PEMFC) fuel cells is to improve the stability of these binary catalysts. Dissolution of the non-precious metal in the acid environment can give rise to a decrease of the activity of the catalysts and to a worsening of cell performance. The purpose of this paper is to provide a better insight into the stability of these Pt–M alloy catalysts in the PAFC and PEMFC environments and the effect of the dissolution of the non-precious metal on the electrocatalytic activity of these materials, in the light of the latest advances on this field. Additionally, the durability of a PtCo/C cathode catalyst was evaluated by a short test in a single PEM fuel cell.

Keywords: PEM fuel cells; Cathode catalysts; Metal dissolution; Durability; Pt–Co alloy

1. Introduction

Low-temperature fuel cells, with either hydrogen (phosphoric acid fuel cell, PAFC, and polymer electrolyte membrane fuel cell, PEMFC) or methanol (direct methanol fuel cell, DMFC) as the fuel, represent an environmentally friendly technology and are attracting considerable interest as a means of producing electricity by direct electrochemical conversion of hydrogen/methanol and oxygen into water/water and carbon dioxide [1,2]. The basic electrode reactions of the PAFC and PEMFC are:

$$H_2 \rightarrow 2(H^+ + e^-) \quad (1)$$

$$\tfrac{1}{2}O_2 + 2(H^+ + e^-) \rightarrow H_2O \quad (2)$$

In the case of the DMFC the electrode reactions are:

$$CH_3OH + H_2O \rightarrow CO_2 + 6(H^+ + e^-) \quad (3)$$

$$\tfrac{3}{2}O_2 + 6(H^+ + e^-) \rightarrow 3H_2O \quad (4)$$

There are, however, severe shortcomings of the present technologies, which need to be overcome to make low-temperature fuel cells more economically attractive. One of the most important problems is related to the low rate of the cathodic reaction where oxygen is reduced. Platinum has the highest catalytic activity for oxygen reduction of any of the pure metals and when supported on a conductive carbon serves as state of the art electrocatalyst in PAFC, PEMFC and DMFC air cathodes [3]. However, due to kinetic limitations of the oxygen reduction reaction (ORR) the cathodic overpotential losses amount to 0.3–0.4 V under typical PEMFC operating conditions [3]. Recently Norskøv et al. [4], using density functional theory calculations, showed that the overpotential of the reactions (2) and (4) can be linked directly to the proton and electron transfer to adsorbed oxygen or hydroxide, which are strongly bonded to the surface at the electrode potential where the overall cathode reaction is at equilibrium. Their model predicts a volcano-shaped relationship between the rate of the cathodic reaction and the oxygen adsorption energy. The model explains why Pt is the best elemental cathode mate-

* Corresponding author. Tel.: +55 16 3373 9899; fax: +55 16 3373 9952.
E-mail address: ernesto@iqsc.usp.br (E.R. Gonzalez).

0378-7753/$ – see front matter © 2006 Elsevier B.V. All rights reserved.
doi:10.1016/j.jpowsour.2006.03.006

rial and why alloying can be used to improve its performance. The development of a more active oxygen reduction electrocatalyst than Pt has been the subject of extensive research for a number of decades. The search for ORR catalysts more active, less expensive and with greater stability than Pt has resulted in the development of Pt-alloys.

The improvement in the ORR electrocatalysis of Pt-alloys has been ascribed to different structural changes caused by alloying, such as modifications in the geometrical (decrease of the Pt–Pt bond distance) [5] or electronic (increase of Pt d-electron vacancy) [6] structure of platinum metal.

Regarding the DMFC, one of the major problems, which decreases the efficiency of conversion of the chemical energy of the methanol fuel to electrical energy, is the methanol crossover through the polymer electrolyte. The problem of methanol crossover in DMFCs has been extensively studied [7–11]: methanol adsorbs on Pt sites in the cathode for the direct reaction between methanol and oxygen. The mixed potential, which results from the oxygen reduction reaction and the methanol oxidation occurring simultaneously, reduces the cell voltage, generates additional water and increases the required oxygen stoichiometric ratio. This problem could be solved either by using electrolytes with lower methanol permeability or by developing new cathode electrocatalysts with both higher methanol tolerance and higher activity for the oxygen reduction reaction than Pt. Higher methanol tolerance is reported in the literature for non-noble metal electrocatalysts based on chalcogenides [12–15] and macrocycles of transition metals [16,17]. These electrocatalysts have shown nearly the same activity for the ORR in the absence as well as in the presence of methanol. However in methanol free electrolytes, these materials did not reach the catalytic activity of dispersed platinum. Developing a sufficiently selective and active electrocatalyst for the DMFC cathode remains one of the key tasks for further progress of this technology. The current direction is to test the activity for the ORR in the presence of methanol of some alloys of the first-row transition metals, which present a higher activity for ORR than platinum in low temperature fuel cell operated on hydrogen.

Carbon supported Pt and Pt–M electrocatalysts are generally used in low temperature fuel cells to enhance the rates of the hydrogen oxidation and oxygen reduction reactions. In such catalysts, the high surface to volume ratio of the metal particles maximizes the area of the surface available for reaction. If the metal particles cannot maintain their structure over the lifetime of the fuel cell, change in the morphology of the catalyst layer from the initial state will result in a loss of electrochemical activity. Indeed, one of the major problems of these catalysts is their stability in the acid environment of PAFC and PEMFC. Pt and M dissolution and Pt sintering are present in PAFCs and, to a less extent, in PEMFCs. It is known that a large part of the non-noble metals is present in the carbon supported Pt-based catalyst in an unalloyed form [18] and that a remarkable dissolution of these non-precious metals in the oxide form occurs in acid environment [19]. As Pt is only slightly soluble in acid environment, the result is an enrichment of Pt on the catalyst surface.

The purpose of this paper is to provide a better insight into the stability of Pt–M alloy catalysts in PAFC and PEMFC environment and the effect of the dissolution of the non-precious metal on the electrocatalytic activity of these materials, in the light of the latest advances on this field. An experimental test on the stability of a carbon supported Pt–Co electrocatalyst, prepared by alloying at high temperature, following 24 h of PEMFC operation is also presented.

2. Experimental

2.1. Preparation of the electrocatalyst

Carbon-supported Pt–Co electrocatalysts were prepared using the following method. The required amount of E-TEK 20 wt.% Pt/Vulcan XC-72 (particle size 2.8 nm) was dispersed in distilled water followed by ultrasonic blending for 15 min. The pH of the solution was raised to 8 with dilute ammonium hydroxide. Stirring was continued during and after the pH adjustment. The required amount of a solution of cobalt chloride ($CoCl_2 \cdot 6H_2O$, Aldrich) was added to this solution. This was followed by the addition of dilute HCl to the solution until a pH of 5.5 was attained. Stirring was continued for 1 h and then the resultant mass was filtered and dried at 90 °C in an air oven for 2 h. Subsequently, the solid was well grinded and the powder was heat-treated at 900 °C in a hydrogen/argon atmosphere for 1 h to form the respective binary alloy catalyst.

2.2. Electrode preparation and test in single PEMFC

To test the electrochemical behavior in a single PEMFC fed with hydrogen/oxygen, these catalysts were used to make two-layer gas diffusion electrodes. A diffusion layer was made with carbon powder (Vulcan XC-72) and 15% (w/w) PTFE and applied over a carbon cloth (PWB-3, Stackpole). A homogeneous water suspension of carbon powder and PTFE was filtered under vacuum onto both faces of the carbon cloth to form the gas diffusion layer of the electrode. On top of this layer, the catalyst was applied in the form of a homogeneous dispersion of Pt–Co/C, or Pt/C, Nafion solution (5%, Aldrich) and 2-propanol (Merck) by a painting procedure. All electrodes were made to contain 0.4 mg Pt cm^{-2}. The Pt loading was determined by weight. The experimental error in the catalyst loading was ±2 wt.%. It was noted that during the painting procedure the platinum loss was about 10 wt.%. To decrease Pt loss, an excess of Pt (10 wt.%) was used in the catalytic ink. After drying, the electrodes were hot-pressed on both sides of a Nafion 115 membrane at 125 °C and 50 kg cm^{-2} for 2 min. Before use, the Nafion 115 membranes were treated with a 3% solution of H_2O_2, washed, and then treated with a 0.5 mol L^{-1} solution of H_2SO_4. The geometric area of the electrodes was 4.62 cm^2, and the anode material was 20% Pt/C E-TEK. The cell temperature was 80 °C and the reagent gases were humidified at 85 °C (oxygen) and 95 °C (hydrogen) and fed to the cell at atmospheric pressure. Before recording the current–potential curves, the single PEMFC was stabilized by operating it at 500 mA cm^{-2} for 2 h. The durability test was performed by operating the PEMFC at 500 mA cm^{-2} for 24 h.

2.3. Energy dispersive X-ray analyses (EDX)

The atomic ratios and the elemental mapping of the Pt–Co/C catalysts were determined by the EDX technique coupled to a scanning electron microscopy LEO Mod. 440 with a silicon detector with Be window and applying 20 keV.

2.4. X-ray diffraction (XRD)

X-ray diffractograms of the catalysts were obtained in a universal diffractometer Carl Zeiss-Jena, URD-6, operating with Cu Kα radiation ($\lambda = 0.15406$ nm) generated at 40 kV and 20 mA. Scans were done at 3° min^{-1} for 2θ values between 20 and 100°.

3. Stability of pure Pt in PAFC and PEMFC environments

In this section we will briefly discuss the dissolution of pure Pt in PAFC and PEMFC environments. At the cathode the problems of Pt dissolution and Pt sintering are present in both PEMFCs and PAFCs. It has to be underlined, however, that the operating environment of the polymer electrolyte fuel cells is not nearly as severe as that of the PAFCs; then a better stability of these alloy catalysts in the PEMFC environment would be expected.

3.1. PAFC conditions

Platinum particle sintering takes place in Pt/C catalysts during operation in PAFCs. Platinum growth rate is high for small particles (<10 nm), likely by the higher solubility in phosphoric acid of edge and corner atoms with respect to ⟨1 1 1⟩ and ⟨1 0 0⟩ atoms, but above 10 nm the size tends to stabilize. Many studies have been devoted to evaluating the mechanism of platinum particle agglomeration in PAFC conditions [20–24]. Essentially, two mechanisms have been proposed to explain the surface area loss of carbon-supported platinum: (1) dissolution/reprecipitation [20–22] of platinum and (2) surface diffusion [23–25]. In the former case, the platinum dissolves in hot phosphoric acid; then, following the saturation of electrolyte with platinum ions, Pt redeposition takes place. The effect of pH of the liquid environment in Pt particle growth was observed by Beard and Ross [26]. They prepared carbon-supported Pt–Co alloys by adding Pt/C catalyst at room temperature into two cobalt solutions, at pH 2 and 11, respectively. When the supported Pt was added into the solution at pH 11, the platinum particle size changed only slightly, while in the case of the solution at pH 2 a remarkable particle growth was observed, from 2.5 to 3.4 nm. Thus, it seems that the acidic solution affects the high-surface-area Pt particle by a dissolution/deposition process since, according to Pourbaix [19], Pt is slightly soluble in acidic environment. As observed by Hyde et al. [27], following 4500 h of cell operating, about 10 wt.% of the platinum was lost from the cathode and migrated across the phosphoric acid to the anode, supporting as a consequence the dissolution/redeposition mechanism. According to Honji et al. [20], Pt particle growth in phosphoric acid is noticeably larger in the presence of air than in the presence of nitrogen. In the latter case, the area loss of supported platinum occurs by surface diffusion of crystallites [23,24] or migration of platinum atoms on the carbon surface [25]. This hypothesis is based on the experimental results of Bett et al. [25]: they found that the nature of the liquid environment seems to have no effect on Pt sintering. Many studies [23,28–35] showed that the resistance to sintering is related to the presence of surface oxygen groups, which interact with the movement of the Pt particles on the carbon surface.

Contradictory results have been reported on the effect of electrode potential on Pt particle growth. Stonehart and Zucks [36] investigated the dependence of the sintering of unsupported platinum on potential. They found that the rate of agglomeration is greatest at low and smallest at high potentials. For that regarding carbon-supported platinum, Bett et al. [25] and Gruver et al. [24] found that the electrode potential has only a small effect on the crystallite growth rate. Honji et al. [20], instead, observed a potential dependence of the Pt sintering. Unlike the results of Stonehart and Zucks regarding Pt black [36], the particle size increases with increasing the potential, particularly at 0.90 V versus reversible hydrogen electrode (RHE).

Finally, the stability of the carbon support also affects the loss of platinum surface area following both platinum particle sintering and platinum release from the carbon support [37–40]. The relation of carbon corrosion and platinum sintering was observed from TEM analysis by Gruver [37]. McBreen et al. [38] showed that Regal 660R carbon with a low volatile content and neutral pH stabilises platinum particles against sintering. Thermal treatment stabilises carbon against the corrosion in hot phosphoric acid [37].

3.2. PEMFC conditions

As previously reported, the acid environment in the PEMFCs is different from that of the PAFCs. The anions of the perfluorinated sulfonic acid polymer are only weakly adsorbed on Pt, in contrast to the phosphoric anions, which are strongly adsorbed. Furthermore, the PEMFCs operates at <100 °C, as compared with the PAFCs, which operates at twice this temperature.

Over the past decade only limited effort has been put into addressing the issue of PEMFC stability and durability. A number of mechanisms can contribute to performance degradation including: catalyst dissolution, catalyst sintering, membrane degradation, and carbon corrosion. A mathematical model has been developed at United Technologies Co. (UTC FC) for the kinetics of platinum dissolution relevant to PEMFCs [41]. Darling and Meyers [41] showed that Pt dissolution in polymer electrolyte fuel cells is negligible at low and high potentials, but is large at intermediate potentials. In their kinetic model of Pt dissolution in PEMFCs, they explained the effect of potential in the following way, by considering three possible reactions:

$$\mathrm{Pt} \rightarrow \mathrm{Pt}^{2+} + 2\mathrm{e}^- \quad \text{(platinum dissolution)} \tag{5}$$

$$\mathrm{Pt} + \mathrm{H_2O} \rightarrow \mathrm{PtO} + 2\mathrm{H}^+ + 2\mathrm{e}^- \quad \text{(platinum oxide film formation)} \tag{6}$$

$$\mathrm{PtO} + 2\mathrm{H}^+ \rightarrow \mathrm{Pt}^{2+} + \mathrm{H_2O} \quad \text{(chemical dissolution of platinum oxide)} \tag{7}$$

Reaction (7) is assumed to be slow, but it is necessary for the model to relax to equilibrium at high potentials when Pt^{2+} and PtO are in equilibrium. The model and experimental data indicated that at lower potentials (i.e. under the conditions of normal H_2/air fuel cell operation), the solubility of platinum in acid is quite low. At higher potentials and on exposure to air to form PtO, the oxide layer effectively insulates the platinum particles from dissolution. At intermediate potentials, however, the uncovered surface is prone to high rates of platinum dissolution.

Recently, Ferreira et al. [42] found that equilibrium concentrations of dissolved platinum species from a Pt/C electrocatalyst sample in 0.5 M H_2SO_4 at 80 °C increase when the applied potential increases from 0.9 to 1.1 V versus RHE. In addition, the platinum surface area loss for a short-stack of PEMFCs operated at open-circuit voltage (∼0.95 V) was shown to be higher than another operated under load (∼0.75 V). Both findings suggest that the formation of soluble platinum species (such as Pt^{2+}) plays an important role in platinum surface loss in PEMFC electrodes.

Mukerjee and Srinivasan [43] evaluated the lifetime in single PEMFC at a constant current density of 200 mA cm^{-2}. Considering the excellent stability of the Dow membrane, the lifetime of the PEMFC essentially depends on the catalyst stability. The cell potential was monitored over a time period of 1200 h. A good stability of cell potential, and, as a consequence, of platinum particles up to 800 h, followed by a slow decrease in the performance of the cell, was observed.

On the other hand, it has been shown that Pt can be found in the membrane after membrane electrode assembly (MEA) aging in a fuel cell, indicating that Pt dissolution can affect the cell performance at regular operating temperatures of a PEMFC [44].

Electrochemical surface oxidation of Vulcan XC-72, a carbon black commonly used in PEM fuel cells, was studied by Kangasniemi et al. [45] following potentiostatic treatments up to 120 h at potentials from 0.6 to 1.2 V at room temperature and 65 °C. They found clear signs of surface oxidation after only 16 h at potentials ≥0.8 V, verifying that surface oxides can be generated under simulated PEM fuel cell conditions. These result suggests that changes in component hydrophobicity, driven by carbon surface oxidation, are an important factor in determining long-term PEMFC performance instability and decay. To overcome this problem, Wang et al. [46] found that multi walled carbon nanotubes show lower loss of Pt surface area and oxygen reduction reaction activity than carbon black Vulcan XC-72, when used as PEM fuel cell catalyst support, as a result of high corrosion resistance.

4. Stability of Pt–M catalysts in PAFC and PEMFC environment

4.1. PAFC conditions

UTC developed carbon supported platinum with base transition metals as V and Cr [47]. By measurements carried out on electrodes with gas diffusion geometry under PAFC conditions the Pt–Cr resulted the more active catalyst. It was reported that in the case of the Pt–V alloy in 99% H_3PO_4, 194 °C and at a potential of 0.9 V reference hydrogen electrode, over 67% of vanadium dissolved, whereas only 37% of the Cr dissolved. Even this loss of the alloying constituent, the activity of the alloy cathodes was higher than pure Pt cathodes with the same amount of Pt. In this patent limited attempts were made to understand this enhancement in activity and in elucidating the state in which the base-metal is present in the catalyst.

The ORR activity of bulk Pt–Cr alloys was investigated by Paffett et al. [48]. They ascribed the improvement of the ORR activity of Pt–Cr catalysts to the dissolution of the passive alloying component, leading to surface roughening and hence increased surface area. Their results show that potential excursions, especially beyond 1.25 V with respect to the reference hydrogen electrode, result in selective depletion of chromium (present as Cr(III) oxide or hydroxide on the surface) as Cr(IV) species in solution. Binary alloys of Pt–Cr with Cr composition <50% have been shown to produce chromium depletion extending two to three monolayers from the surface. The bulk alloys richer in chromium have been shown to suffer a much greater depletion with a platinum enriched zone capable of extending up to 100 nm from the surface.

Beard and Ross [26] investigated the ORR activity under PAFC conditions of carbon supported Pt–Co alloy catalysts in the form of fuel cell electrodes. They prepared Pt–Co/C catalysts starting from commercial Pt/C (10% Pt) by two methods. A method (Series A) consisted in the preparation of an acidic (pH 2 by addition of HCl) $Co(OH)_2$ solution in water/methanol, followed by Pt/C addition into this solution. In the other method (Series B) Pt/C was added into a basic (pH 11 by addition of NH_4OH) $Co(NO_3)_2$ solution in water/methanol. In both cases the Pt:Co atomic ratio was 3:1. Three thermal treatments at 700, 900 and 1200 °C under inert atmosphere were performed on each catalyst. In both series in the absence of thermal treatment the catalyst has a lattice parameter, obtained from XRD, indicative of pure Pt. Following thermal treatments in Series A the lattice parameter decreased with increasing heating temperature, indicative of alloy formation. As shown in Table 1, the results of X-ray fluorescence indicated a significant effect of alloying on Co dissolution during tests in PAFC. Both the as-prepared (not heat-treated) catalysts lost in excess of 80% of the cobalt present, whereas in Series B the catalyst treated at 1200 °C lost 30%, with the Series A 1200 °C sample (higher degree of alloying than Series B 1200 °C) losing only 15%. Loss of cobalt in the phosphoric acid environment was the lowest among alloyed catalysts examined, particularly when the Pt_3Co ordered phase was

Table 1
XRD lattice parameters of Pt–Co catalysts before and after a duration test in PAFC and Co loss determined by X-ray fluorescence [26]

Sample	Pt (wt.%)	Lattice parameter before test (nm)	Lattice parameter after test (nm)	Co loss (%)
Series A as-prepared	9.2	0.3295	0.3919 (0.3833)	82.2
Series A 1200 °C	8.8	0.3864	0.3866 (0.3833)	15.0
Series B as-prepared	9.2	0.3927	0.3907 (0.3828)	87.5
Series B 1200 °C	8.9	0.3910	0.3904 (0.3834)	28.4

present. From the known solubilities of cobalt oxides in strong acids [19], loss of unalloyed cobalt is not surprising, but some cobalt was lost from the alloy phase as well. The post test XRD analyses indicated that in each of the four tested catalysts one phase had a lattice parameter close to that of Pt_3Co (0.3831 nm), with the second phase being close to pure Pt. Indeed, the majority of cobalt remaining in the catalyst was an alloy with Pt_3Co composition, suggesting that this ordered alloy may have sufficient stability in PAFC conditions to be of practical interest. They ascribed the slight improvement of activity of the Pt–Co catalysts with respect to pure Pt to some roughness effects, like those reported by Paffett et al. [48] for bulk Pt–Cr alloys, for surfaces dealloyed by corrosion of the base-metal or to the particle termination primarily in ⟨1 0 0⟩ vicinal planes (⟨1 0 0⟩ vicinal planes are more active than ⟨1 1 1⟩). Studies performed in parallel on Pt–Co bulk alloys [49] showed that, when heated in oxygen at fuel cell temperatures, the surface region is dealloyed by oxidation to form a cobalt oxide overlayer. The oxide overlayer dissolves in hot concentrated phosphoric acid, leaving a dealloyed pure Pt surface region on top of the bulk alloy.

Beard and Ross [50] subjected carbon supported Pt–Ti catalysts, thermally treated at various temperatures, to stability tests in phosphoric acid at standard fuel cell operating conditions, 98% acid, 170 °C, potentials in the range of 0.6–0.9 V, in the form of gas diffusion electrodes. The results indicated loss of titanium in all the catalysts. The loss of Ti after the electrochemical testing was much lower for the sample heated at the highest temperature (1200 °C), indicating some stabilization of Ti by alloying. They found that Pt_3Ti alloy crystallites are stable in H_3PO_4 at fuel cell air cathode conditions, provided the alloy crystallites are sufficiently large (>20 nm), with the surface, however, devoid of Ti. Smaller alloy crystallites, instead, appeared unstable, with phase separation by Ti dissolution.

In a study on the ORR activity of carbon supported Pt–Co alloys with Pt:Co atomic ratio 55:45 in PAFC conditions, Watanabe et al. [51] observed higher activity on the alloys than on Pt. They found that the ordered Pt–Co structure presents 1.35 higher mass activity compared to the disordered alloy. Moreover, they demonstrated that both Pt and Co dissolve out preferentially from small-size alloy particles and Pt redeposits on the surface of large-size ones in hot H_3PO_4. The observed decay in the performance of the alloy catalysts was explained by the leaching of the alloyed non-precious metal to the electrolyte. Indeed, as shown in Fig. 1, about 30% of the Co dissolved within a very short time, 1–2 h, at 0.8 V and 210 °C in hot H_3PO_4, and then the dissolution slowed down. According to the authors, the loss of Co at the initial stage may be attributed to the dissolution of Co atoms present on the surface of the alloy crystallites, and the subsequent slow loss may be due to that of the Co present in the interior of the crystallite, since the inside atoms do not diffuse out quickly. The alloy with a disordered crystallite structure, which is more corrosion-resistant than an ordered one, maintains higher electrocatalytic activity for a longer time. Regarding the effect of atomic ordering on the stability of Pt–Co alloy catalysts in PAFC conditions, it has to be pointed out that Beard and Ross [26], as previously reported, found an opposite result.

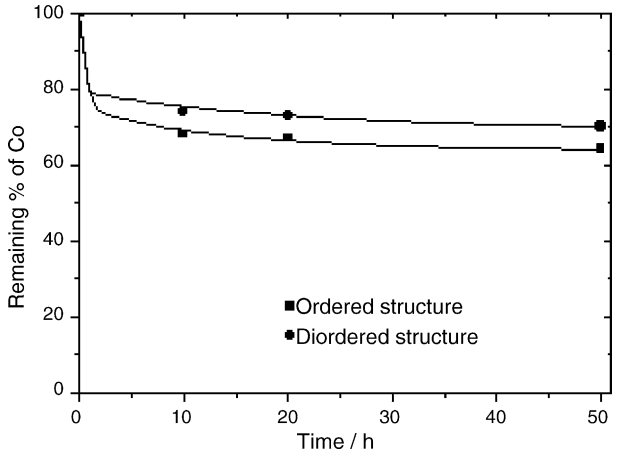

Fig. 1. Changes of the remaining contents of Co in the ordered and disordered alloys with corrosion time at 210 °C in 105% H_3PO_4. Reproduced from Ref. [51], Copyright (1994), by permission of The Electrochemical Society Inc.

It was found in PAFC durability evaluations that the base element of the Pt-alloy gradually leached out over thousands of hours of normal fuel cell operation. The initial Pt-alloys were prepared using carbothermal reduction (mixing a pre-formed Pt/C catalyst with the oxide of a chosen base-metal followed by heat treatment to 800–1000 °C in an inert atmosphere), that resulted in a solid solution and in which rapid quenching of the smaller crystallites impeded them from forming true equilibrium structures [52]. To rectify the problem, new catalysts were prepared by subjecting them to a slow annealing to produce ordered structures that were found to be stable for 9000 h at 205 °C [53].

4.2. PEMFC conditions

4.2.1. Literature survey

As well analysed by Gasteiger et al. [54], there are at least three possible causes for the leaching of base-metal from a Pt-alloy/C catalyst in PEMFCs: (i) excess base-metal deposited onto the carbon support during preparation, (ii) incomplete alloying of the base element to Pt due to a low alloying temperature applied during formation of the alloy, (iii) even a well-alloyed base-metal may leach out of the surface under PEMFC operating conditions and leave a Pt-enriched surface or skin since thermodynamically base-metals are unstable under PEMFC potentials in acidic electrolytes (even Pt-alloys do not have high enough heats of mixing to confer stability).

Mukerjee and Srinivasan [43] investigated durability and stability of carbon supported Pt_3Cr, Pt_3Co and Pt_3Ni alloy catalysts in PEMFCs. The lifetime studies on these catalysts under PEMFC operational conditions showed only negligible losses in performance over periods of 400–1200 h, as can be seen in Fig. 2. In this time range a high stability of the ratio between the amount of the alloying component and the amount of Pt in the catalyst was observed.

By XPS measurements, Toda et al. [6] found that most of the Ni, Co or Fe easily disappeared from all the Pt-alloy surface layers, probably by dissolution, by submitting the surface to an anodic potential of 1.1 V, even in diluted acid solution, at

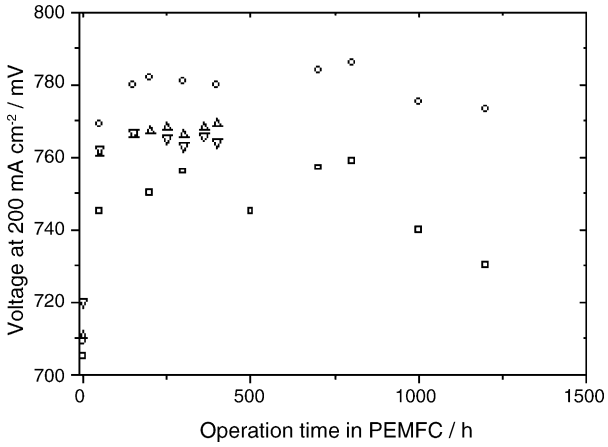

Fig. 2. Lifetime evaluation of carbon supported Pt and Pt-alloy electrocatalysts for oxygen reduction in PEMFCs. Current density 200 mA cm^{-2}, cell temperature 50 °C, ambient pressure. (□) Pt; (◯) PtCr; (△) PtNi; (▽) PtCo. Reprinted from Ref. [43], Copyright (1993), with permission from Elsevier.

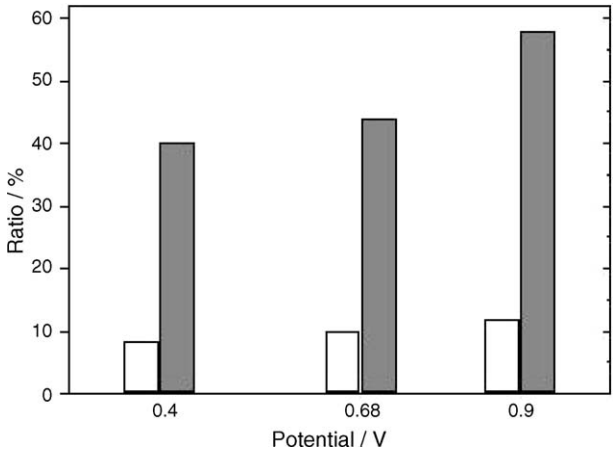

Fig. 3. Bar plot comparing the loss in activity with loss in alloying material under steady state conditions. Reprinted from Ref. [56], Copyright (2004) with permission from Elsevier.

room temperature. However, the alloy compositions determined with EDX analysis did not show apparent differences before and after the electrochemical experiments. Also, negligible differences were observed in the XRD patterns before and after electrochemical tests. These results indicate that the loss of the base-metal only occurs within few monolayers of the alloy surface. The modification of the electronic structure of this Pt layer with respect to that of the bulk alloys gives rise to an enhancement of the ORR. The ORR activity of these catalysts decreased when the temperature was raised above 60 °C and settled to almost the same values as the Pt electrode [55]. This behaviour was probably due to the thickening of the Pt skin-layer by considerable dissolution of the non-precious metal components (Fe, Co, Ni) from the alloys.

Colon-Mercado et al. [56] evaluated the catalytic, corrosion and sintering properties of commercial Pt/C and Pt_3Ni/C catalysts using an accelerated durability test (ADT). The ADT cell consists of a three-electrode system, which includes a reference electrode, a platinum mesh counter electrode and the catalyst-coated gas diffusion layer (GDL) as a working electrode. For the ADT, the electrodes were immersed in a 0.3 M H_2SO_4 solution, which mimics the environment of the electrode–membrane interface on the cathode side. Unlike the case of an electrode–membrane assembly (MEA) interface, in which only the catalyst in contact with the membrane is active, in the case of the ADT the entire active surface area of the catalyst is exposed to protons, since the electrode is completely immersed in the electrolyte. Under this specific condition, the deterioration of the catalysts is accelerated. The degree of alloying of the Pt_3Ni catalyst was not indicated. They found that the total amount of Ni dissolved depends on the applied potential, and increases from 8.3 to 12% when the potential increases from 0.4 to 0.9 V versus the standard hydrogen electrode. A strong correlation between the amount of Ni dissolved and the oxygen reduction activity of the catalyst was observed. The increase of both the Ni loss and the ORR activity loss with increasing the potential is shown in Fig. 3. Moreover, the carbon supported Pt_3Ni alloy showed better resistance to sintering than a pure platinum catalyst. According to the authors, the mobility of platinum on a carbon surface is hindered when Ni is present; thus, the sintering effect of platinum atoms is suppressed. Similar results have been observed by Wei et al. [57] for Pt–Fe alloy on a carbon substrate and by Salgado et al. [58] for carbon supported Pt–Co alloys. The same authors [59] investigated the stability of different Pt–M (M = Fe, Co and Ni) alloy catalysts both using ADT and in PEM fuel cell tests. Also in this work a strong correlation between the amount of the alloying component dissolved and the ORR activity of the binary alloy catalysts was observed. Fig. 4 shows the dissolution rate estimated for different Pt-alloy catalysts at 0.8 V versus NHE. The highest metal loss was estimated for the samples with a Pt to non-noble metal ratio of 1:1. As expected, the metal loss in the samples with a Pt to non-noble metal ratio of 3:1 is lower than that estimated for a Pt:M ratio of 1:1. In case of a Pt:M ratio of 1:1, the Pt–Ni alloy shows the lowest metal dissolution. Cross-sectional studies by electron microprobe analysis of the membrane electrode assembly after fuel cell testing revealed cobalt dissolution by diffusion into the membrane.

On the other hand, Park et al. [60] observed no dissolution of Ni in the bulk Pt–Ni (1:1) alloy nanoparticle catalyst

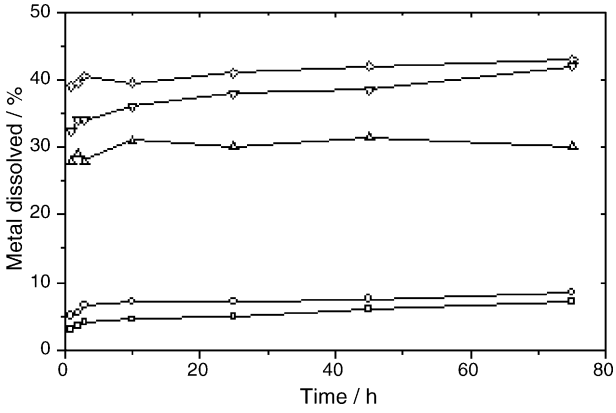

Fig. 4. Non-noble metal dissolution data as a function of time for the different Pt-alloy catalysts at a potential of 0.8 V vs. NHE. (□) Pt_3Ni; (◯) Pt_3Co; (△) PtNi; (▽) PtFe; (◊) PtCo. Reprinted from Ref. [59], Copyright (2005) with permission from Elsevier.

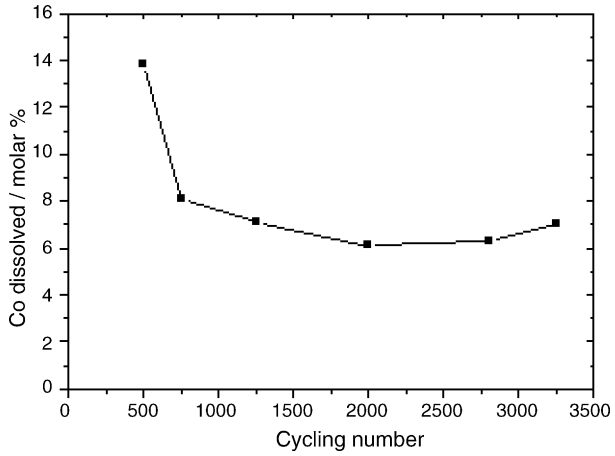

Fig. 5. Cobalt dissolution as a function of cycle number of PtCo electrode in 0.1 M $HClO_4$. The cycling test was conducted at 25 °C. Reprinted from Ref. [61], Copyright (2005) with permission from Elsevier.

in 2.0 mol L^{-1} CH_3OH + 0.5 mol L^{-1} H_2SO_4 in the potential range of 0–1.6 V versus NHE. Although some dissolution of Ni could take place, the amount dissolved from the Pt lattice was apparently very small. According to the authors, this indeed implies that the metallic state of nickel is either passivated by Ni hydroxides or exists as a stable phase within the platinum lattice.

Yu et al. [61] evaluated the durability of a Pt–Co cathode catalyst in the Pt:Co atomic ratio 2.5:1 in a dynamic fuel cell environment with continuous water fluxing on the cathode. Fig. 5 presents the Co^{2+} concentration as a function of cycling number. It is noted that 13.9 mol% cobalt dissolved in the first 400 cycles. The amount of cobalt dissolution was reduced subsequently and leveled off to approximately 6% after 800 cycles. This result was coincidental with a high performance loss in the first 400 cycles and a reduced loss in subsequent cycles. The results indicated that cobalt dissolution neither detrimentally reduces the cell voltage nor dramatically affects the membrane conductance. The overall performance loss over 2400 cycles of the PtCo/C membrane electrode assemblies (MEAs) was less than that of the Pt/C MEA. The performance losses of the Pt/C MEA over 1200 cycles mainly resulted from the cathode electrochemical area (ECA) loss due to platinum recrystallization, while the performance losses of the PtCo/C MEA resulted from the activity loss due to cobalt dissolution as well as the ECA loss.

Gasteiger et al. [54] proposed a pre-leaching of the alloy to minimize the contamination of the MEA during operation owing to Co dissolution. They investigated the durability of the baseline on Pt/C and multiply leached Pt–Co/C MEAs tested in a short stack. They observed that the enhancement or performance offset of 15–25 mV between the Pt/C and the Pt_xCo_{1-x}/C is maintained throughout the 1000 h of stack operation within limits of error. They also observed that the degradation rate of the Pt/C and Pt-alloy/C MEAs are comparable at about 50 and 60 mV h^{-1}. The MEAs stayed essentially stable throughout the duration of testing indicating no degradation of the membrane due to contamination. The surface area loss for the PtCo/C catalyst was lower than that for Pt/C measured over the 1000 h of operation. These results indicated that the Pt-alloy catalyst starts life with a larger particle size and does not sinter as rapidly as Pt/C.

Bonakdarpour et al. [62] studied the dissolution of Fe and Ni from $Pt_{1-x}M_x$ (M = Fe, Ni) catalyst under simulated operating conditions of PEMFCs. Electron microprobe measurements showed that transition metals are removed from all compositions during acid treatment, but that the amount of metal removed increases with x, acid strength and temperature. For low M content ($x < 0.6$) the dissolved transition metals originated from the surface, while for $x > 0.6$ the transition metals dissolved also from the bulk. XPS results indicated complete removal of surface Ni(Fe) after acid treatment at 80 °C for all compositions.

Protsailo and Haug [63] investigated the performance and, most importantly, durability improvement of PEMFCs, that can be achieved using Pt–Co/C and PtIrCo/C, synthesized by the carbothermal technique. The alloys showed not only better activity compared to pure Pt, but also remarkable durability in the conditions at which Pt alone is prone to dissolution. The losses of the real surface area of Pt/C, PtCo/C and PtIrCo/C following 1800 cycles at 120 °C were about 45% for Pt/C, 18% for PtCo/C and 8% for PtIrCo/C, respectively.

Considerable work has been carried out by Johnson Matthey between 1995 and 1997 [64,65] on carbon supported binary alloys such as PtFe, PtMn, PtNi, PtCr, and PtTi alloys with a Pt:M atomic ratio of 50:50 and heat-treated to various temperatures. Electron probe microanalysis (EPMA) was employed to evaluate the stability of the alloys during operation in small PEMFCs. The Cr and Ti alloys did not show any apparent leaching from the catalyst to the membrane or anode catalyst layer while the PtFe, PtMn, and PtNi all showed leaching of the base-metal into the MEA, but no performance loss was observed over the 200 h of testing.

Xiong and Manthiram [66] investigated the ORR activity of carbon supported Pt–M alloys (M = Fe, Co, Ni and Cu) in PEMFC. They did not observe any significant performance loss in the polarization studies carried out for two consecutive days.

Yang et al. investigated the ORR activity of carbon supported PtNi [67] alloy catalysts prepared by a Pt–carbonyl route. They observed that the real surface area of Pt in the Pt–Ni alloy catalysts before and after the electrochemical polarization at 0.80 V for 1 h in oxygen-saturated perchloric acid solution increases only by ca. 3.5%, indicating that the stability of the alloy catalyst is good and that no Pt surface enrichment on the alloy catalysts occurs during the ORR. Thus, it is believed that the Pt/Ni surface composition keeps almost a constant value during the electrochemical measurements.

Paulus et al. [68] investigated the oxygen reduction kinetics on commercial carbon supported Pt–Ni and Pt–Co alloy catalysts using the thin film rotating ring disk electrode (RRDE) method in 0.1 M $HClO_4$ in the temperature range between room temperature and 60 °C. Pt–Co in the atomic ratio 3:1 and 1:1 and Pt–Ni in the ratio 3:1 were stable during the experiments. However, unlike the other catalysts, the base voltammogram of Pt:Ni 1:1 changed substantially over the whole time of the experiment, particularly after the measurements carried out above room temperature. These changes showed that the base voltammogram

becomes more "Pt-like", which is probably indicative of leaching of Ni from the surface.

Xie et al. [69] investigated the long-term durability of hydrogen–air polymer electrolyte fuel cells. They found that chromium in a Pt_3Cr binary alloy catalyst migrates from cathode to anode during the course of life testing when operating within the oversaturated, or high-humidity, gas feed regime. The same research group [70] monitored the morphological changes occurring in membrane electrode assemblies (MEAs) during the course of the life testing of H_2/air PEFCs. They found that the Pt anode catalyst was less stable than the Pt_3Cr cathode catalyst under high current density and high humidity conditions, which was confirmed by the higher extent of migration observed for the pure Pt than for the Pt_3Cr material. Some Pt particles (from both electrodes) were found to migrate into the membrane during the testing period.

Li et al. [71] prepared a carbon supported Pt–Fe catalyst by a modified polyol synthesis method in an ethylene glycol solution, followed by heat-treatment under H_2/Ar (10 vol.%) at moderate temperature (300 °C, Pt–Fe/C300). This catalyst was tested as cathode in a direct methanol fuel cell. EDX analysis indicated a Pt:Fe atomic ratio of 93:7. The lattice parameter of Pt–Fe/C300 was 0.3912 nm, while the lattice parameters of pure platinum and the Pt_3Fe alloy were 0.3924 and 0.3865 nm, respectively. At the treatment temperature of 300 °C, Fe cannot alloy completely with Pt and is more prone to corrode during the DMFC operations at 90 °C. Pt–Fe/C300 exhibited higher ORR activity and better performance than other Pt–Fe/C or Pt/C catalysts when employed as cathode material in direct methanol single cell tests. The authors confirmed the presupposition that the Fe^{3+} ion can promote the ORR activity by rotating disk electrode (RDE) measurements adding some Fe^{3+} ion in the $HClO_4$ solution. The mass activity for the Pt/C catalyst in 1.0 M $HClO_4$ + 100 ppm Fe^{3+} electrolyte was 13.4 mA mg^{-1} Pt at 660 mV (SCE), which is higher than that of Pt/C in 1.0 M $HClO_4$ (9.3 mA mg^{-1} Pt). It was also found that the limiting currents for the Pt/C catalyst increased considerably when 100 ppm Fe^{3+} were added in the $HClO_4$ electrolyte. Sun and Tseung account the Fe^{3+} promotion effect on ORR activity for Pt/C to the higher H_2O_2 decomposition activity when Fe^{3+} and Pt/C are co-present [72]. EDX analysis showed that the Pt:Fe ratio increases from 93:7 to 95:5 after a 40 h DMFC test, which means near 30 at.% of Fe content loss during the test. Also according to the authors, the improvement in the performance of Pt–Fe/C for oxygen reduction may be partly due to the higher peroxide decomposition activity of Pt in presence of dissolved Fe.

Shukla et al. [73] prepared carbon supported Pt–Fe by alloying at 750 °C for 1 h under flowing hydrogen followed by annealing for 12–15 h in the same environment. EDX analysis indicated a Pt:Fe atomic ratio of 54:46. While the XRD pattern for the Pt/C catalyst indicates a face centered cubic phase [74], the XRD pattern for the Pt–Fe/C catalyst resembles an ordered face centered tetragonal phase [75]. It has been documented that annealing of Pt–Fe catalysts results in conversion from a disordered face centered cubic phase to a chemically ordered face centered tetragonal phase [75]. There was little difference in the XRD patterns of the Pt–Fe/C alloy sample prior to and after exposing it to 0.5 M aqueous H_2SO_4. As observed from atomic absorption spectroscopic data shown in Fig. 6, only 0.6 ppm of Fe leached from the alloy sample during the first 4 h, and there was no leaching subsequently, suggesting that the as-prepared Pt–Fe alloy sample has some free iron present in it. In this case, the authors ascribed the enhanced performance in DMFC using the Pt–Fe/C catalyst to the higher proportion of active platinum sites in relation to Pt/C, and a completely different nearest neighbour environment in the Pt–Fe/C catalyst where, unlike the Pt/C catalyst, the nearest neighbour sites are occupied by Fe, which helps to scavenge impurities from the neighbouring active platinum sites.

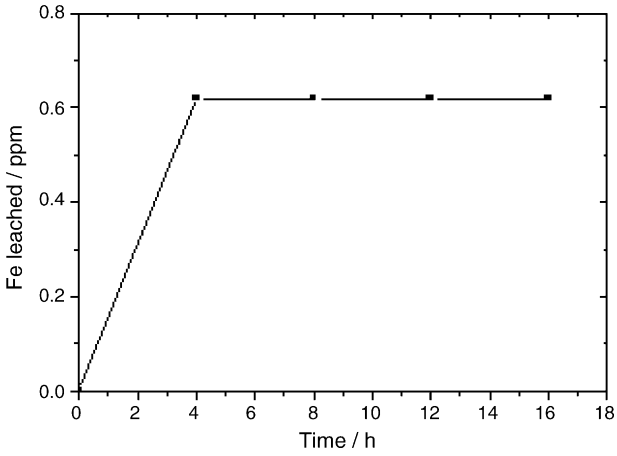

Fig. 6. Amount of Fe leached from the as-prepared Pt–Fe/C alloy sample on soaking it in 0.5 M aqueous H_2SO_4 for 16 h at 85 °C as observed by atomic absorption spectroscopy. Reprinted from Ref. [73], Copyright (2004) with permission from Elsevier.

The results of the different tests on the stability of Pt–M alloy catalysts in PAFC and PEMFC conditions and the consequences on the electrocatalytic activity and cell performance are summarized in Scheme 1.

4.2.2. *Short duration tests of Pt–Co/C electrocatalysts in PEMFC*

The choice of a Pt:Co composition of 75:25 was based on its high activity for the ORR. The ORR activity of Pt–M (M = first row transition metals) catalysts goes trough a maximum that depends on the Pt–Pt bond distance and the Pt d-band vacancy [76]. In the case of Pt–Co the optimal values of these parameters are obtained with a Pt:Co composition of about 75:25.

Table 2
EDX composition of the carbon supported Pt–Co electrocatalyst before and after the 24 h duration test in a PEMFC

Status	Sample	Pt:Co (at.%)		Pt:Co:C (wt.%)		
		Pt	Co	Pt	Co	C
Before PEMFC test	1	73.58	26.42	20.86	2.74	76.41
	2	73.42	26.58	22.18	2.78	75.04
	3	75.07	24.93	23.23	2.73	74.04
After PEMFC test	1	84.82	15.42	16.38	1.19	82.44
	2	81.14	18.86	20.00	1.67	78.33
	3	79.70	20.30	19.21	1.96	78.83

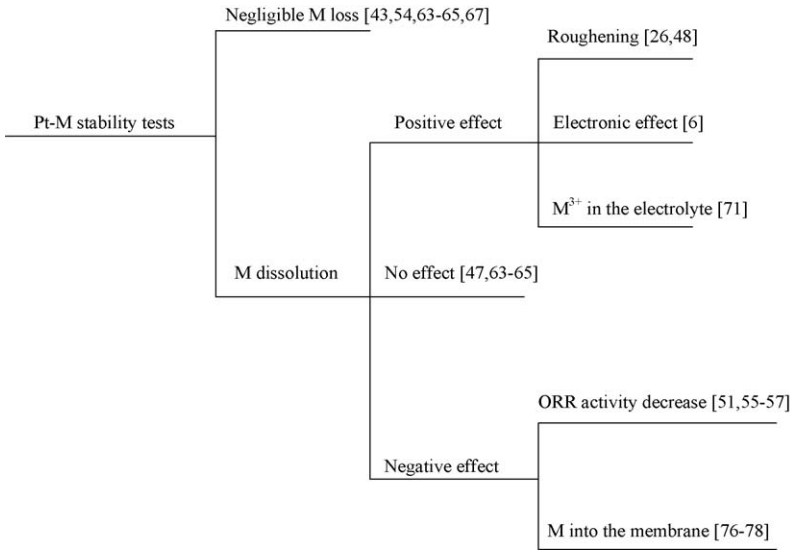

Scheme 1. Reference based scheme of the stability of Pt–M alloy catalysts in acid fuel cell environment.

The Pt–Co actual compositions were characterized by EDX measurements on several different regions of each sample of the carbon supported Pt–Co particles before and after the 24 h test in a single PEMFC. Table 2 gives the EDX results of carbon supported Pt–Co particles on three different regions. Following PEMFC test, the average Pt:Co composition went from 74:26 to 82:18. Then, loss of cobalt occurred during the test. A loss of platinum, to a less extent than cobalt, was also detected.

The results of the analysis of elemental mapping, before and after the duration test in the PEMFC, are shown in Figs. 7a–d and 8a–d, respectively. It can be seen that the metals are uniformly distributed on the carbon surface. By comparing Fig. 7d (before the test) and Fig. 8d (after the test) it can be observed that the amount of cobalt is lower following the test in the single cell.

Fig. 9 shows the XRD patterns of the binary catalyst before (Fig. 9a) and after (Fig. 9b) the duration test in the PEMFC. No change in the XRD pattern of Pt–Co/C catalyst following cell operation was observed. The Pt:Co alloy composition, calculated by the lattice parameter (0.3841 nm) through the relationship reported in Ref. [58] was 80:20 before and after the test, in good agreement with the value of the EDX composition. Then, From EDX and XRD analysis it can be inferred that all non-alloyed Co was lost. The loss of non-alloyed Co was fast:

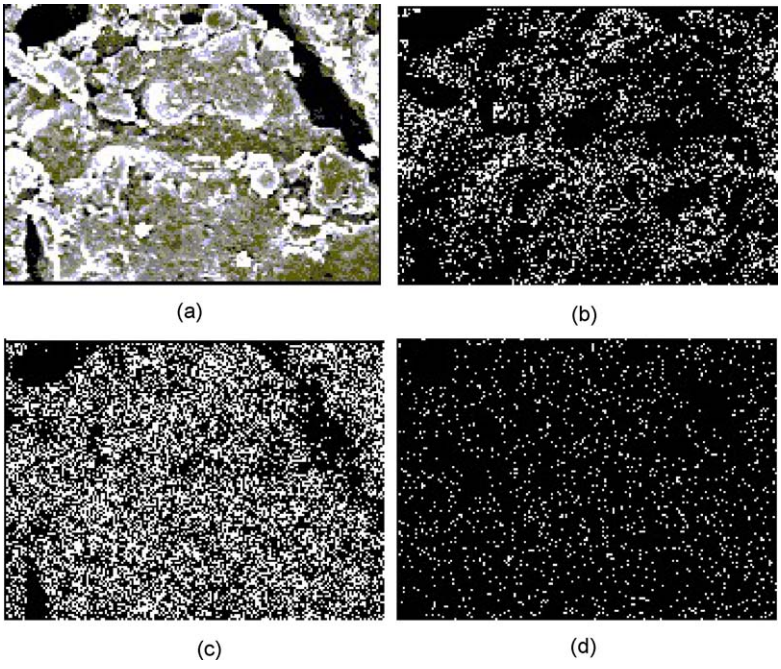

Fig. 7. Elemental mapping on $Pt_{75}Co_{25}$/C catalyst before a test in single PEMFC: (a) general morphology; (b) carbon; (c) platinum and (d) cobalt. Resolution 9 k×.

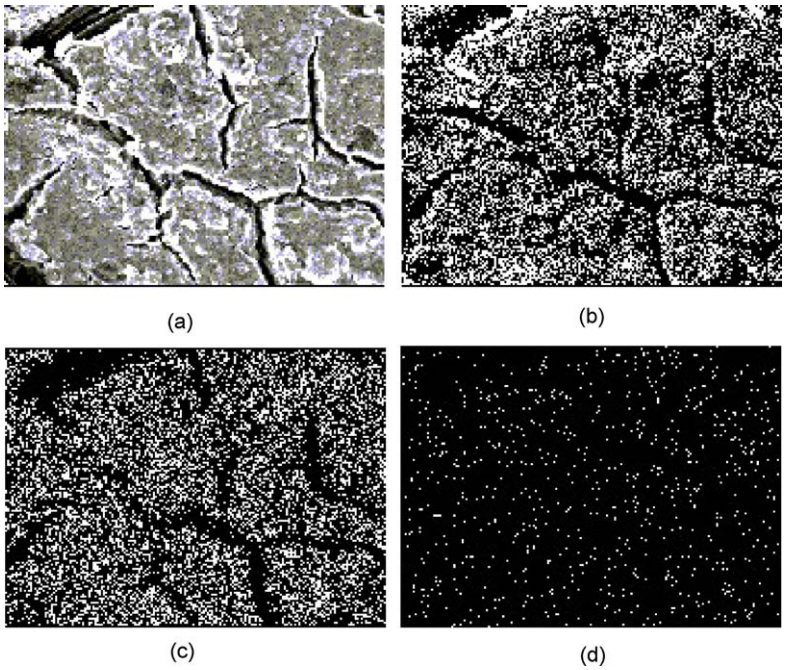

Fig. 8. Elemental mapping on $Pt_{75}Co_{25}$/C catalyst after a 24 h test in single PEMFC: (a) general morphology; (b) carbon; (c) platinum and (d) cobalt. Resolution 9 k×.

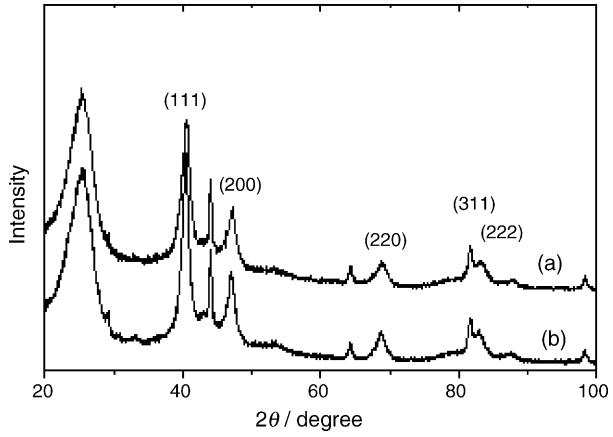

Fig. 9. XRD pattern of the Pt–Co/C catalyst before (a) and after (b) the 24 h test in PEMFC.

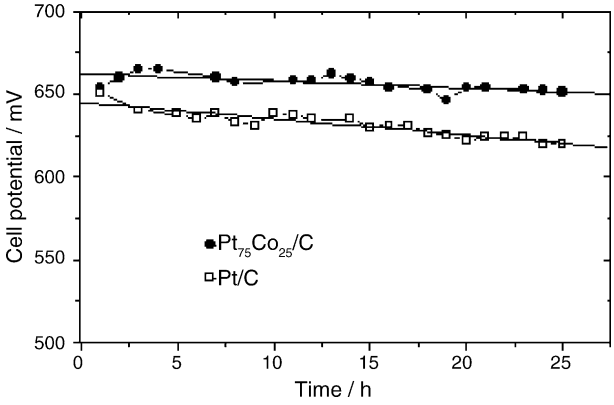

Fig. 10. Dependence of the potential at 500 mA cm^{-2} of a single PEMFC with Pt/C and Pt–Co/C as cathode material on operational time.

after 24 of test in PEMFC almost all of non-alloyed cobalt disappeared. The alloyed cobalt, instead, was retained in the Pt crystal structure.

Fig. 10 shows the dependence of the potential at 500 mA cm^{-2} of the single fuel cell with Pt/C and Pt–Co/C as cathode material on operational time. The cell with Pt–Co/C as cathode catalyst presented a more stable performance than Pt. As can be seen in Fig. 10, the degradation rate of Pt/C (0.98 mV h^{-1}) was more than twice than that of Pt–Co/C (0.44 mV h^{-1}). These results agree with the higher stability of Pt–Co/C electrocatalysts in PEMFC duration tests found by Gasteiger et al. [54] and Protsailo and Haug [63].

5. Conclusions

Both high and low stability of platinum based binary catalysts in acid medium have been reported in the literature. Some authors reported high stability of the catalysts after more than 1000 h of duration tests in PEM fuel cells [43,54]. On the other hand, a poor stability of the materials was found following short duration (few hours) measurements in half cells [55,68].

Certainly, the type of the test influences the different stability of these catalysts: half cell tests can lead to different results than fuel cell tests. Also, parameters such as temperature, pressure, pH, type of acid and duration of the test affect the behaviour of the binary catalysts.

According to some authors [47,64,65,68], the stability of non-noble metals in acid environment depends on the type of metal: Pt–Cr and Pt–Co are usually considered more stable than Pt–V, Pt–Ni and Pt–Fe. We think, instead, that the stability of these catalysts depends on the degree of alloying and, to a less extent, on the metal particle size, and not on the kind of M. Generally,

Cr and Co present a higher degree of alloying with Pt than V, Ni and Fe: this could explain the higher stability in acid medium of Pt–Cr and Pt–Co than Pt–V, Pt–Ni and Pt–Fe. The results of different works indicate that the most part of M dissolved came from non-alloyed M.

The metal particle size of the binary alloys also influences the dissolution of the base-metal in acid environment. Higher stability of Pt–M alloys with large particle sizes than that of catalysts with small particle sizes was observed [50,51]. Therefore, bulk alloys present higher stability against dissolution than supported high surface area alloys.

Conflicting results on the effect of the ordered structure of the alloy on its stability in acid environment have been reported [50,51], so this matter has to be more deeply investigated.

A better resistance of alloy particles to sintering than that of pure platinum particle was observed [54,56–58]. The presence of the non-precious metal seems to hinder the mobility of platinum on the carbon.

The base-metal dissolution can affect the characteristics of the catalyst in two opposite ways. The non-precious metal loss from the catalyst can increase the ORR activity of the cathode material by surface roughening (large amount of metal dissolution) [48], and hence increased Pt surface area, or by modification of the electronic structure of the Pt skin layer originating from the base-metal loss (very small amount of metal dissolution) [6]. On the other hand, the loss of alloyed non-noble metal leads to a decrease of the ORR activity and the methanol resistance of the catalyst due to loss of the beneficial structural modifications of Pt metal by alloying.

In the case of PEM fuel cells, the contamination of the membrane by cationic impurities has detrimental effects on membrane properties with regard to conductivity, water management and durability. Metal cations from the dissolution of the catalyst can easily exchange with a proton of the membrane/ionomer because of a stronger affinity of metal cations than protons with the sulfonic group. Exchange of metal cations with the sulfonic group might affect the performance of the fuel cell giving rise to a decrease in the ionomer/membrane conductivity [77], a dehydration of the membrane [78], and a lowering of the oxygen reduction kinetics by a decrease of oxygen concentration or oxygen diffusion coefficient in the ionomer film [79].

Tests in half cells are important to evaluate the electrochemical characteristics of a catalyst, but it has to pointed out that, from the practical point of view, the test in fuel cell is the ultimate evaluation criterion for novel materials. The working conditions such as temperature, pressure and fuel flows are crucial to determine the real performance of a system. In this regard, duration tests in PEMFCs indicated a positive effect of the presence of the non-precious metal on the stability of the catalyst [43,54,63–65].

On this basis, the use of alloyed Pt–M catalysts as cathode materials in low temperature fuel cells is recommended. In addition to a higher activity for oxygen reduction and a higher methanol tolerance, these catalysts present a higher stability against dissolution than the state-of-the-art pure platinum cathodes.

Acknowledgements

The authors thank the Conselho Nacional de Desenvolvimento Científico e Tecnológico (CNPq, Proc. 300477/2005-8), FAPESP, MCT and CAPES for financial assistance to the project.

References

[1] P. Costamagna, S. Srinivasan, J. Power Sources 102 (2001) 242.
[2] X. Ren, P. Zelenay, S. Thomas, J. Davey, S. Gottesfeld, J. Power Sources 86 (2000) 111.
[3] S. Gottesfeld, T.A. Zawodzinski, Polymer electrolyte fuel cells, in: R.C. Alkire, H. Gerischer, D.M. Kolb, C.W. Tobias (Eds.), Advances in Electrochemical Science and Engineering, vol. 5, 1st ed., Wiley-VCH, Weinheim, 1997, p. 195.
[4] J.K. Norskøv, J. Rossmeisl, A. Logadottir, L. Lindqvist, J.R. Kitchin, T. Bligaard, H. Jonsson, J. Phys. Chem. B 108 (2004) 17886.
[5] V. Jalan, E.J. Taylor, J. Electrochem. Soc. 130 (1983) 2299.
[6] T. Toda, H. Igarashi, H. Uchida, M. Watanabe, J. Electrochem. Soc. 146 (1999) 3750.
[7] B. Gurau, E.S. Smotkin, J. Power Sources 112 (2002) 3339.
[8] P.M. Urban, A. Funke, J.T. Muller, M. Himmen, A. Docter, Appl. Catal. A Gen. 221 (2001) 459.
[9] A. Heinzel, V.M. Barragan, J. Power Sources 84 (1999) 70.
[10] K. Ramya, K.S. Dhathathreyan, J. Electroanal. Chem. 542 (2003) 109.
[11] J. Cruickshank, K. Scott, J. Power Sources 70 (1998) 40.
[12] B. Schubert, H. Tributsch, N. Alonso-Vante, A. Perrin, J. Catal. 112 (1988) 384.
[13] B. Schubert, N. Alonso-Vante, E. Gocke, H. Tributsch, Ber. Bunsenges Phys. Chem. 92 (1988) 1279.
[14] N. Alonso-Vante, H. Tributsch, Nature 323 (1996) 431.
[15] T.J. Schmidt, U.A. Paulus, H.A. Gasteiger, N. Alonso-Vante, R.J. Behm, J. Electrochem. Soc. 147 (2000) 2620.
[16] R. Jiang, D. Chu, J. Electrochem. Soc. 147 (2000) 4605.
[17] P. Convert, C. Coutanceau, P. Crouigneau, F. Gloaguen, C. Lamy, J. Appl. Electrochem. 31 (2001) 945.
[18] E. Antolini, Mater. Chem. Phys. 78 (2003) 563.
[19] M. Pourbaix, Atlas of Electrochemical Equilibrium in Aqueous Solutions, 1st ed., Pergamon Press, Bristol, England, 1966.
[20] A. Honji, T. MoriI, K. Tamura, Y. Hishinuma, J. Electrochem. Soc. 135 (1988) 355.
[21] A.C.C. Tseung, S.C. Dhara, Electrochim. Acta 20 (1975) 681.
[22] P. Bindra, S. Clouser, E. Yeager, J. Electrochem. Soc. 126 (1979) 1631.
[23] K.F. Blurton, H.R. Kunz, D.R. Rutt, Electrochim. Acta 23 (1978) 183.
[24] G.A. Gruver, R.F. Pascoe, H.R. Kunz, J. Electrochem. Soc. 127 (1980) 1219.
[25] J.A. Bett, K. Kinoshita, P. Stonehart, J. Catal. 41 (1976) 124.
[26] B.C. Beard, P.N. Ross, J. Electrochem. Soc. 137 (1990) 3368.
[27] P.J. Hyde, C.J. Maggiore, S. Srinivasan, J. Electroanal. Chem. 168 (1984) 383.
[28] F. Coloma, A. Sepulveda-Escribano, J.L. Fierro, F. Rodriguez-Reinoso, Langmuir 10 (1994) 750.
[29] G.C. Torres, E.I. Iablonski, G.T. Baronetti, A.A. Castro, S.R. de Miguel, O.A. Scelza, M.D. Blanco, M.A. Pena Jimenez, J.L.G. Fierro, Appl. Catal. A 161 (1997) 213.
[30] M.C. Roman-Martinez, D. Cazorla-Amoros, A. Linares-Solano, C.S.M. Lecea, Carbon 33 (1995) 3.
[31] S.R. Miguel, O.A. Scelza, M.C. Roman-Martinez, C.S.M. Lecea, D. Cazorla-Amoros, A. Linares-Solano, Appl. Catal. A 170 (1998) 93.
[32] C. Prado-Burguete, A. Linares-Solano, F. Rodriguez-Reinoso, C.S.M. Lecea, J. Catal. 115 (1989) 98.
[33] D.J. Suh, T.J. Park, S.K. Ihm, Carbon 31 (1993) 427.
[34] P. Ehrburger, O.P. Majahan, P.L. Walker, J. Catal. 43 (1976) 61.
[35] A. Guerrero-Ruiz, P. Badenes, I. Rodriguez-Ramos, Appl. Catal. A 173 (1998) 313.

[36] P. Stonehart, P.A. Zucks, Electrochim. Acta 17 (1972) 2333.
[37] G.A. Gruver, J. Electrochem. Soc. 125 (1978) 1719.
[38] J. McBreen, H. Olender, S. Srinivasan, K. Kordesch, J. Appl. Electrochem. 11 (1981) 787.
[39] P. Stonehart, Carbon 22 (1984) 423.
[40] M. Uchida, Y. Aoyama, M. Tanabe, N. Yanagihara, N. Eda, A. Ohta, J. Electrochem. Soc. 142 (1995) 2572.
[41] R. Darling, J. Meyers, J. Electrochem. Soc. 150 (2003) A1523.
[42] P.J. Ferreira, G.J. la O', Y. Shao-Horn, D. Morgan, R. Makharia, S. Kocha, H.A. Gasteiger, J. Electrochem. Soc. 152 (2005) A2256.
[43] S. Mukerjee, S. Srinivasan, J. Electroanal. Chem. 357 (1993) 201.
[44] T. Patterson, Proceedings of the AlChE National Conference, New Orleans, LA, Spring, 2002.
[45] K.H. Kangasniemi, D.A. Condit, T.D. Jarvi, J. Electrochem. Soc. 151 (2004) E125.
[46] X. Wang, W. Li, Z. Chen, M. Waje, Y. Yan, J. Powe Sources 158 (2006) 154–159.
[47] D.A. Landsman, F.S. Luczak, US Patent 4,316,944 (1982).
[48] M.T. Paffett, J.G. Berry, S. Gottesfeld, J. Electrochem. Soc. 135 (1988) 1431.
[49] U. Bardi, B. Beard, P.N. Ross, J. Vac. Sci. Technol. A 6 (1988) 665.
[50] B.C. Beard, P.N. Ross, J. Electrochem. Soc. 133 (1986) 1839.
[51] M. Watanabe, K. Tsurumi, T. Mizukami, T. Nakamura, P. Stonehart, J. Electrochem. Soc. 141 (1994) 2659.
[52] V. Jalan, D.A. Landsman, US Patent 4,186,944 (1980).
[53] F.J. Luczak, D.A. Landsman, US Patent 4,677,092 (1987).
[54] H.A. Gasteiger, S.S. Kocha, B. Sompalli, F.T. Wagner, Appl. Catal. B 46 (2005) 9.
[55] N. Wakabayashi, M. Takeichi, H. Uchida, M. Watanabe, J. Phys. Chem. B 109 (2005) 5836.
[56] H.R. Colon-Mercado, H. Kim, B.N. Popov, Electrochem. Commun. 6 (2004) 795.
[57] Z. Wei, H. Guo, Z. Tang, J. Power Sources 62 (1996) 233.
[58] J.R.C. Salgado, E. Antolini, E.R. Gonzalez, J. Phys. Chem. B 108 (2004) 17767.
[59] H.R. Colon-Mercado, B.N. Popov, J. Power Sources 155 (2006) 253–263.
[60] K. Park, J. Choi, B. Kwon, S. Lee, Y. Sung, H. Ha, S. Hong, H. Kim, A. Wieckowski, J. Phys. Chem. B 106 (2002) 1869.
[61] P. Yu, M. Pemberton, P. Plasse, J. Power Sources 144 (2005) 11.
[62] A. Bonakdarpour, J. Wenzel, D.A. Stevens, S. Sheng, T.I. Monchesky, R. Lobel, R.T. Atanasoski, A.K. Schmoeckel, G.D. Vernstrom, M.K. Debe, J.R. Dahn, J. Electrochem. Soc. 152 (2005) A61.
[63] L. Protsailo, A. Haug, Electrochemical Society Meeting Abstracts, 208th ECS Meeting, Los Angeles, CA, 2005 (abs. 1023).
[64] D. Thompsett, in: W. Vielstich, H. Gasteiger, A. Lamm (Eds.), Handbook of Fuel Cells—Fundamentals, Technology and Applications, vol. 3, Wiley, Chichester, UK, 2003, p. 467 (Chapter 37).
[65] T.R. Ralph, J.E. Keating, N.J. Collis, T.I. Hyde, ETSU Contract Report F/02/00038, 1997.
[66] L. Xiong, A. Manthiram, J. Electrochem. Soc. 152 (2005) A697.
[67] H. Yang, W. Vogel, C. Lamy, N. Alonso-Vante, J. Phys. Chem. B 108 (2004) 11024.
[68] U.A. Paulus, A. Wokaun, G.G. Scherer, T.J. Schmidt, V. Stamenkovic, N.M. Markovic, P.N. Ross, J. Phys. Chem. B 106 (2002) 4181.
[69] J. Xie, D.L. Wood, D.M. Wayne, T.A. Zawodzinski, P. Atanassov, R.L. Borup, J. Electrochem. Soc. 152 (2005) A104.
[70] J. Xie, D.L. Wood, K.L. More, R.L. Borup, J. Electrochem. Soc. 152 (2005) A104.
[71] W. Li, W. Zhou, H. Li, Z. Zhou, B. Zhou, G. Sun, Q. Xin, Electrochim. Acta 49 (2004) 1045.
[72] Z. Sun, A.C. Tseung, Electrochem. Solid State Lett. 3 (2000) 413.
[73] A.K. Shukla, R.K. Raman, N.A. Choudhury, K.R. Priolkar, P.R. Sarode, S. Emura, R. Kumashiro, J. Electroanal. Chem. 563 (2004) 181.
[74] A.K. Shukla, M. Neergat, P. Bera, V. Jayaram, M.S. Hegde, J. Electroanal. Chem. 504 (2001) 111.
[75] S. Sun, C.B. Murray, D. Weller, L. Folks, A. Moser, Science 287 (2000) 1989.
[76] S. Mukerjee, S. Srinivasan, M.P. Soriaga, J. McBreen, J. Electrochem. Soc. 142 (1995) 1409.
[77] M.J. Kelly, G. Fafilek, J.O. Besenhard, H. Kronberger, G.E. Nauer, J. Power Sources 145 (2005) 249.
[78] T. Okada, Y. Ayato, M. Yuasa, I. Sekine, J. Phys. Chem. B 103 (1999) 3315.
[79] T. Okada, Y. Ayato, H. Satou, M. Yuasa, I. Sekine, J. Phys. Chem. B 105 (2001) 6980.